

Proton and Ion Linear Accelerators

2. Introduction to Accelerating Structures

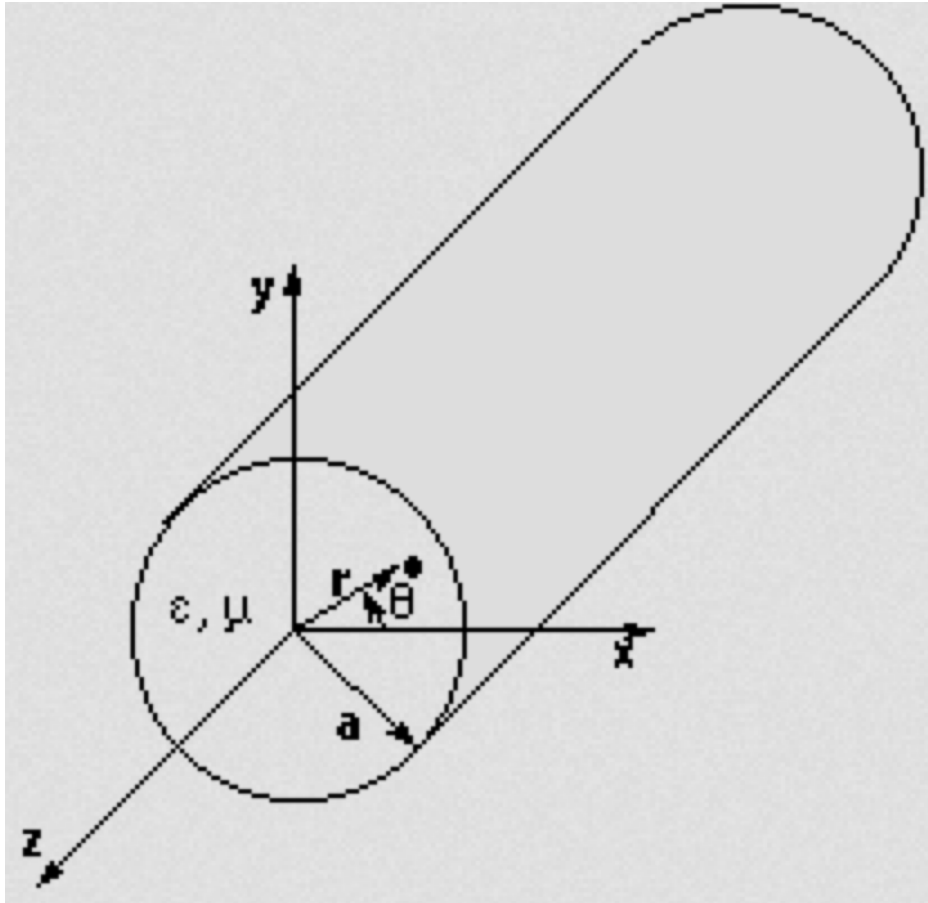
Yuri Batygin

Los Alamos National Laboratory

U.S. Particle Accelerator School

July 15 - July 26, 2024

Waves in Uniform Circular Waveguide



Circular waveguide.

Wave equations

$$\Delta \vec{E} - \frac{1}{c^2} \frac{\partial^2 \vec{E}}{\partial t^2} = 0$$

$$\Delta \vec{B} - \frac{1}{c^2} \frac{\partial^2 \vec{B}}{\partial t^2} = 0$$

Waves in Uniform Circular Waveguide (cont.)

Wave equation for electrical field

$$\Delta \vec{E} - \frac{1}{c^2} \frac{\partial^2 \vec{E}}{\partial t^2} = 0$$

Wave equation for E_z component in cylindrical coordinates

$$\frac{1}{r} \frac{\partial}{\partial r} \left(r \frac{\partial E_z}{\partial r} \right) + \frac{1}{r^2} \frac{\partial^2 E_z}{\partial \theta^2} + \frac{\partial^2 E_z}{\partial z^2} - \frac{1}{c^2} \frac{\partial^2 E_z}{\partial t^2} = 0$$

The solution is for TM wave:

$$E_z = R(r)\Theta(\theta)Z(z)T(t)$$

$$T(t) = T_0 e^{-i\omega t} \quad \Theta(\theta) = \Theta_0 e^{-in\theta} \quad Z(z) = Z_0 e^{ik_z z}$$

$$\frac{d^2 R}{dr^2} + \frac{1}{r} \frac{dR}{dr} + \left(\frac{\omega^2}{c^2} - k_z^2 - \frac{n^2}{r^2} \right) R = 0$$

Transverse wave number

$$k_r^2 = \frac{\omega^2}{c^2} - k_z^2$$

Wave equation can be rewritten

$$\frac{d^2 R}{d(k_r r)^2} + \frac{1}{(k_r r)} \frac{dR}{d(k_r r)} + \left(1 - \frac{n^2}{(k_r r)^2} \right) R = 0$$

Solution: Bessel function

$$R = A J_n(k_r r)$$

Waves in Uniform Circular Waveguide (cont.)

Longitudinal component vanishes at the boundary of cavity

$$E_z(a) = 0 \quad J_n(k_r a) = 0$$

Transverse wave number is determined as

$$k_r a = v_{nm}$$

v_{nm} is the root of equation $J_{nm}(x)=0$

$$k_r = \frac{v_{nm}}{a}$$

Traveling wave in uniform waveguide

$$E_z = E_o J_n\left(v_{nm} \frac{r}{a}\right) \cos n\theta e^{-(\omega t - k_z z)}$$

Wave number $k_z = \frac{2\pi}{\lambda}$ and wavelength

$$k_z^2 = \frac{\omega^2}{c^2} - \frac{v_{nm}^2}{a^2} \quad \lambda = \frac{2\pi}{k_z}$$

Cut-off frequency $k_z = 0$:

$$\omega_c = c \frac{v_{nm}}{a}$$

Phase of the wave

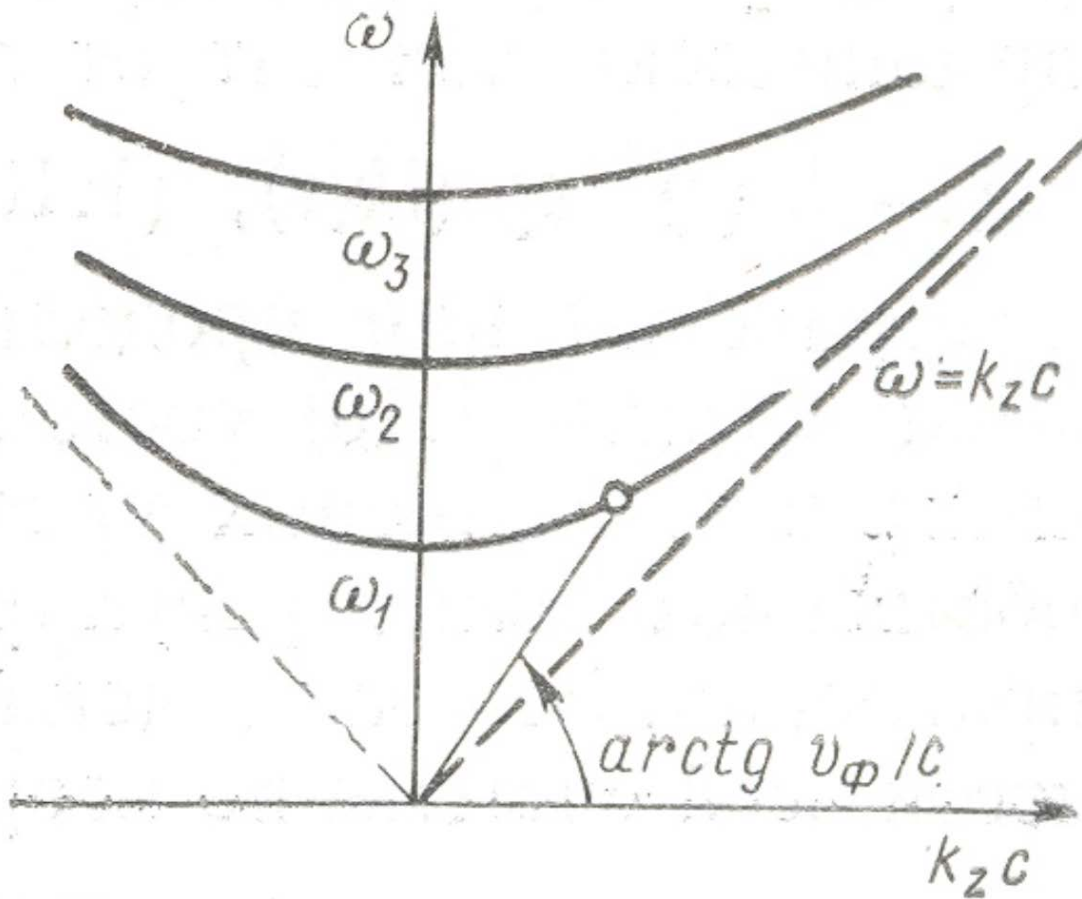
$$\varphi = \omega t - k_z z$$

Phase velocity: $d\varphi/dt=0$

$$v_{ph} = \frac{\omega}{k_z} = \frac{c}{\sqrt{1 - \left(\frac{\omega_c}{\omega}\right)^2}} > c$$

In uniform waveguide phase velocity is always larger than velocity of light

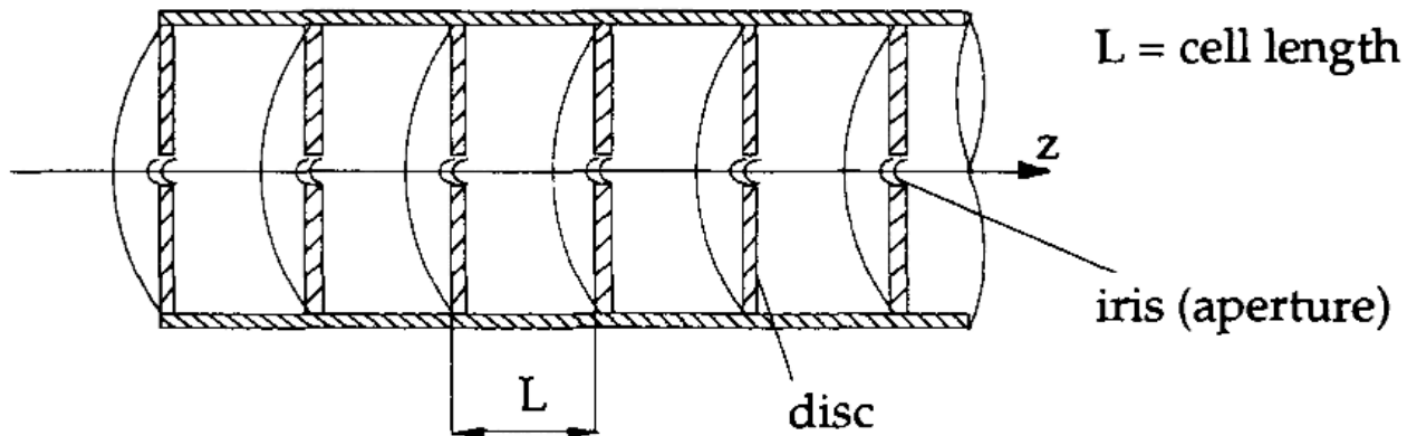
Dispersion Diagram of Uniform Waveguide



$$\omega^2 = c^2 \left(k_z^2 + \frac{v_{nm}^2}{a^2} \right)$$

Dispersion (Brilouin) diagram

Traveling Wave Accelerating Structures



Longitudinal electric field with periodic conditions

$$E_z(r, z, t) = F(r, z)e^{j(\omega t - k_0 z)} \quad F(r, z + L) = F(r, z)$$

Expansion in Fourier series

$$F(r, z) = \sum_n a_n(r) e^{-j(2\pi n/L)z}$$

Substitution into wave Equation

$$e^{j\omega t} \sum_n e^{-j(k_0 + 2\pi n/L)z} \left[\frac{d^2 a_n(r)}{dr^2} + \frac{1}{r} \frac{da_n(r)}{dr} + K_r^2 a_n(r) \right] = 0$$

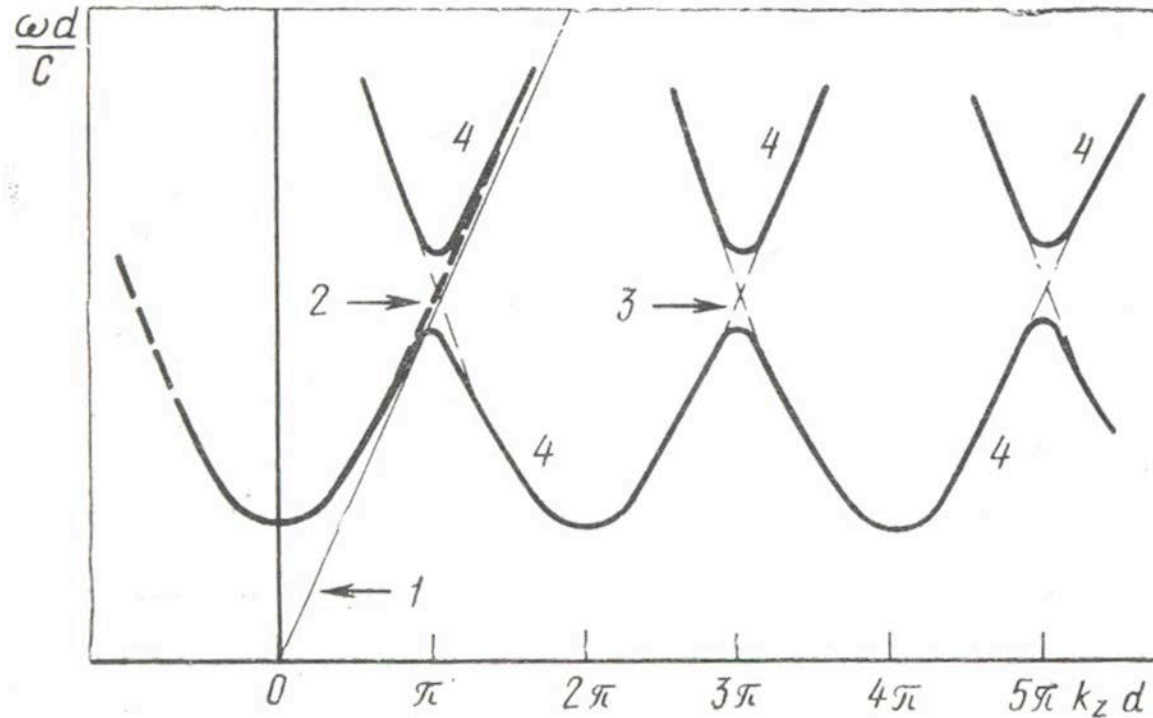
Transverse wave number

$$K_r^2 = \left(\frac{\omega}{c} \right)^2 - \left[k_0 + \frac{2\pi n}{L} \right]^2$$

Phase velocity

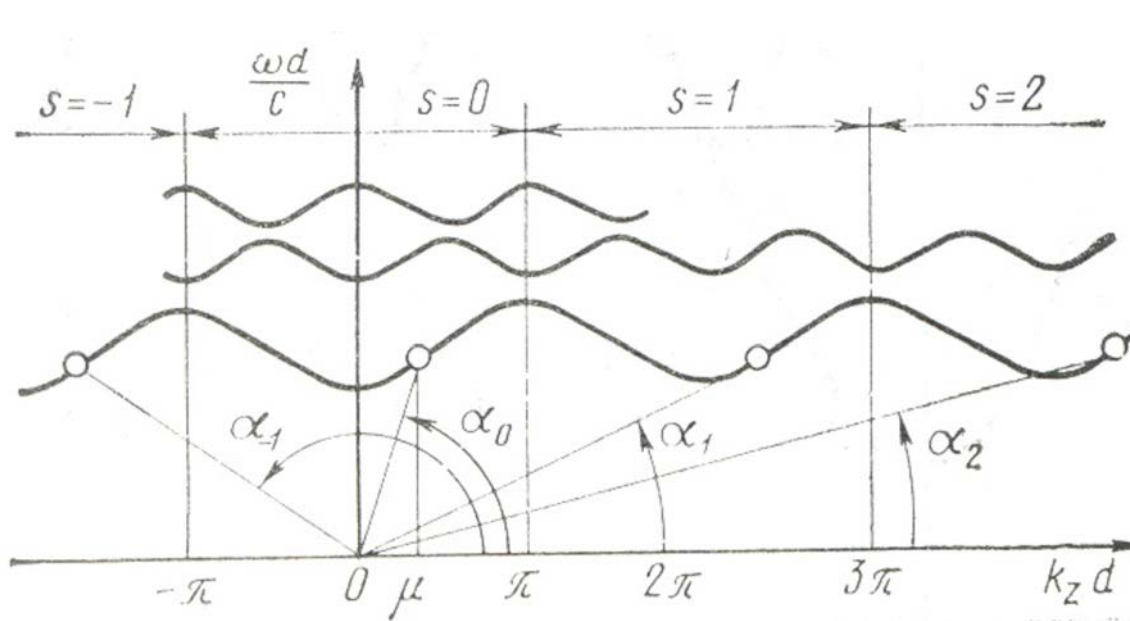
$$v_{ph} = \frac{\omega}{k_0 + 2\pi n/L} = \frac{\omega}{k_n}$$

Dispersion Diagram of Periodic Waveguide

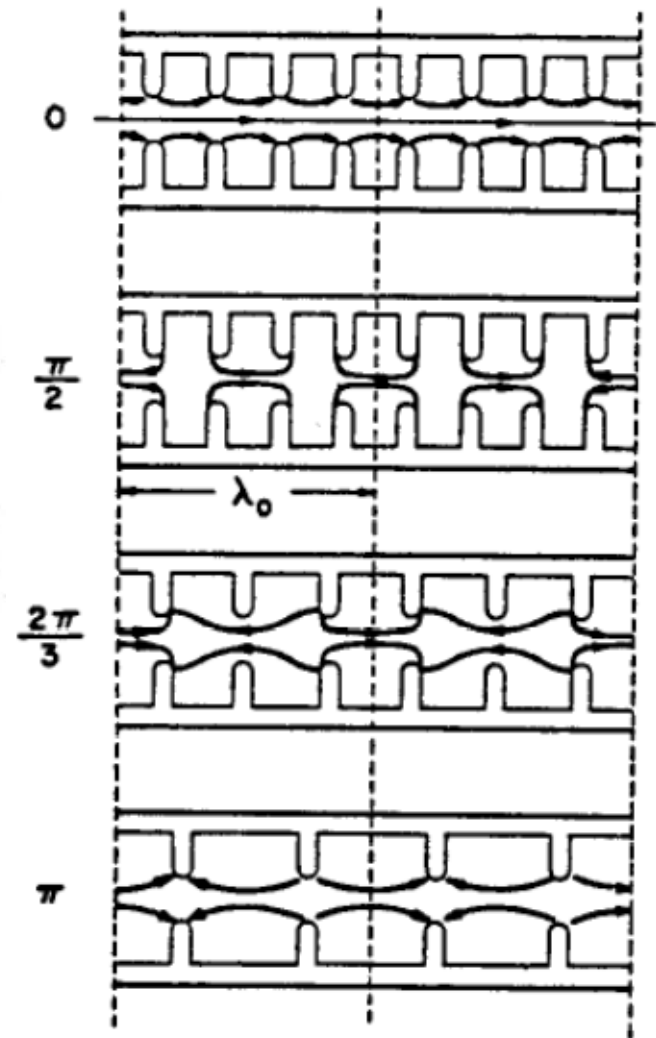


Dispersion diagram of periodic structure is a combination of diagrams for uniform waveguide periodically repeated after one period of the structure.

Traveling Wave Accelerating Structures

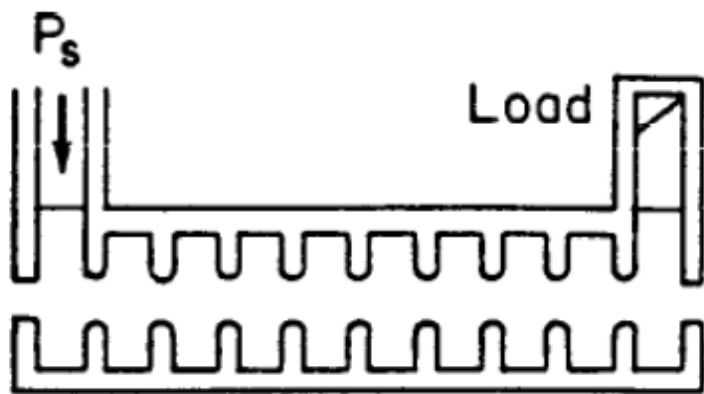


Brillouin diagram for disk-loaded waveguide. Angles α_1 , α_2, \dots correspond to phase velocities of various space harmonics.



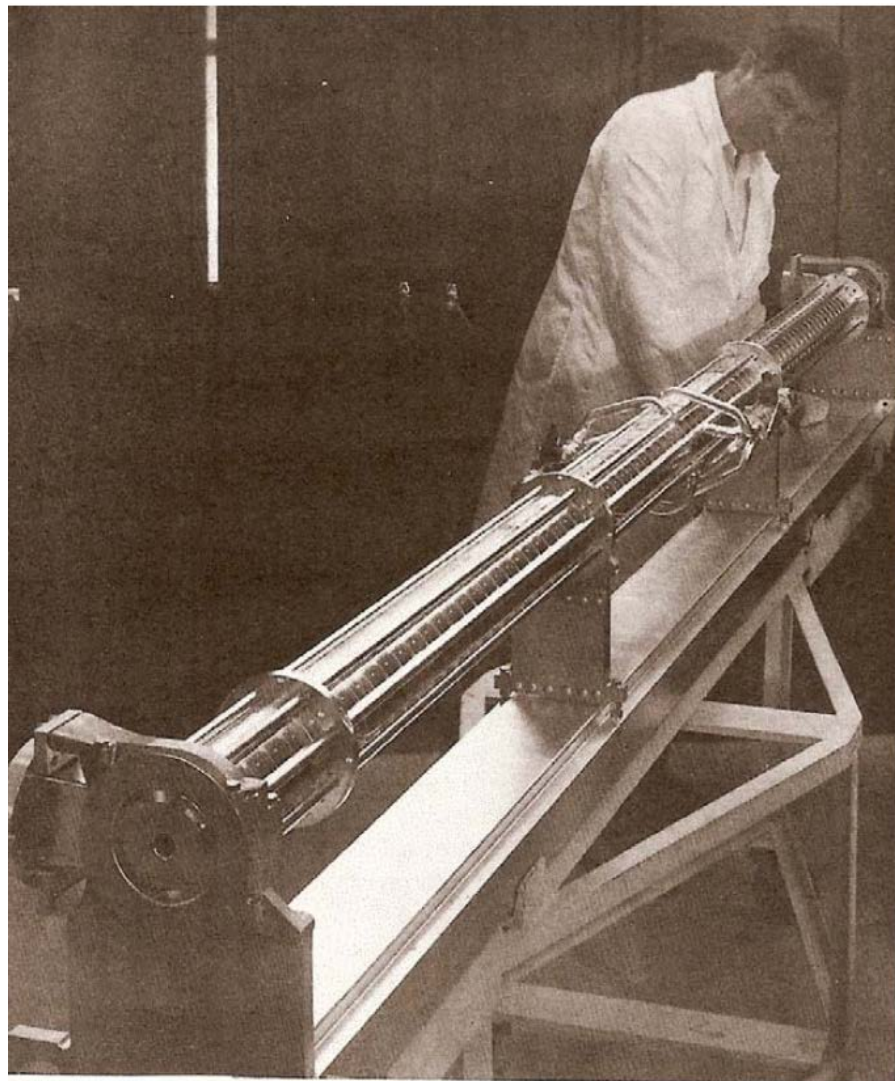
Snapshots of electric field configurations for disk-loaded structures with various phase shifts per period.

Traveling Wave Accelerating Structures

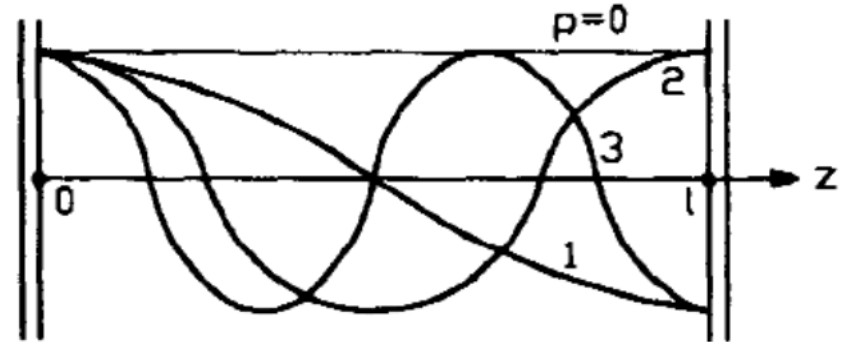
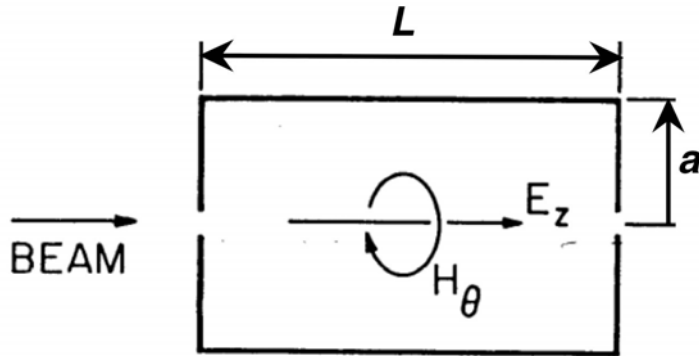


Linac with traveling wave. Primarily used for electrons.

SLAC accelerating structure: 10-foot disk-loaded, 2856 MHz, 86 cells per structure, 960 structures make up the SLAC 3-km linac.



Cylindrical Resonator



Longitudinally integer number of half-variations can be excited

Transverse boundary condition:

$$k_z = \frac{\pi p}{L}$$

$$E_z(a) = 0 \quad J_n(k_r a) = 0 \quad k_r = \frac{v_{nm}}{a}$$

$$\frac{\omega_o^2}{c^2} - k_z^2 = \frac{v_{nm}^2}{a^2}$$

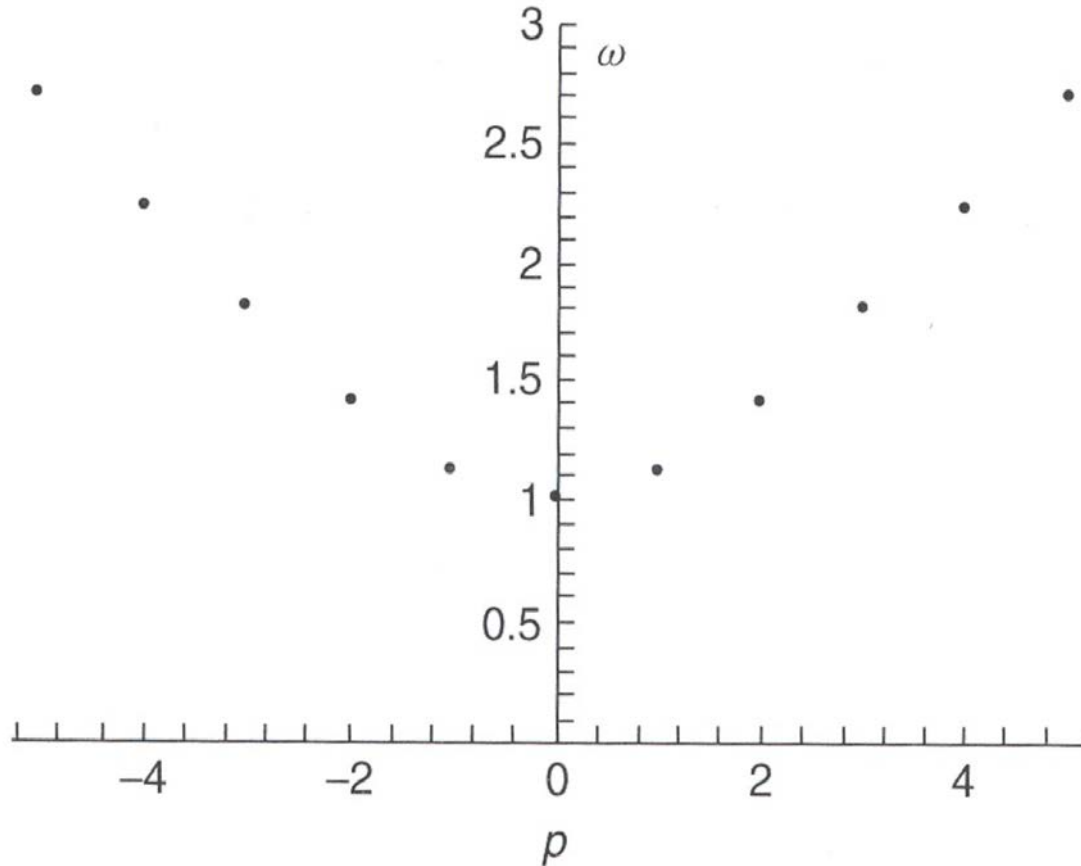
Frequency of oscillation mode is

$$\omega_o = c \sqrt{\frac{v_{nm}^2}{a^2} + \left(\frac{\pi p}{L}\right)^2}$$

Longitudinal component

$$E_z = E_o J_n\left(v_{nm} \frac{r}{a}\right) \cos n\theta \cos \frac{\pi p z}{L}$$

Dispersion Diagram for Cylindrical Cavity



Dispersion curve for the TM_{01p} family of modes of a cylindrical circular cavity.

TM_{nmp} Modes in Cylindrical Cavity

Field components of TM_{nmp} modes in cylindrical cavity

$$E_z = E_o J_n(\chi r) \cos n\theta \cos \chi_z z$$

$$E_r = -E_o \frac{\chi_z}{\chi} J'_n(\chi r) \cos n\theta \sin \chi_z z$$

$$E_\theta = E_o \frac{n\chi_z}{\chi^2 r} J_n(\chi r) \sin n\theta \sin \chi_z z$$

$$H_r = -iE_o \frac{n\omega_o \epsilon_o}{\chi^2 r} J_n(\chi r) \sin n\theta \cos \chi_z z$$

$$H_\theta = -iE_o \frac{\omega_o \epsilon_o}{\chi} J'_n(\chi r) \cos n\theta \cos \chi_z z$$

$$H_z = 0$$

n – number of variation in azimuthal angle θ

m – number of variation in radius r

P – number of variation in longitudinal direction z

$$\chi = \frac{v_{nm}}{a} \quad \chi_z = \frac{\pi p}{L}$$

Example: TM_{010} Mode in Cylindrical Cavity

Field components

$$E_z = E_o J_o\left(\nu_{01} \frac{r}{a}\right) \cos \omega_o t$$

$$B_\theta = -\frac{E_o}{c} J_1\left(\nu_{01} \frac{r}{a}\right) \sin \omega_o t$$

Boundary condition

$$E_z(a) = 0$$

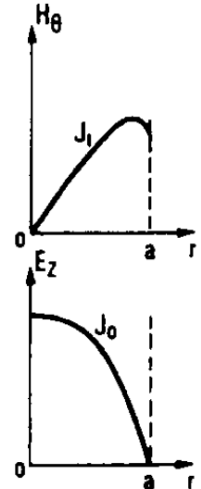
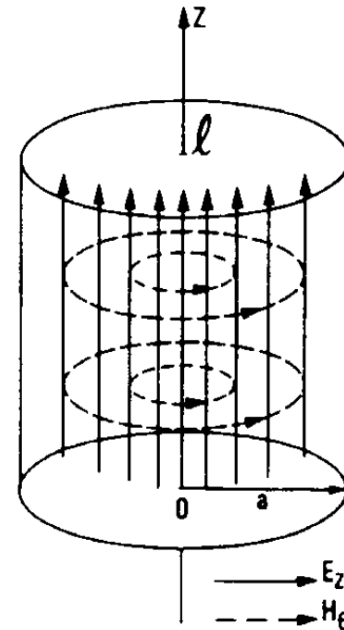
$$\nu_{01} = 2.405$$

Frequency of resonator

$$k_z = 0$$

$$\omega_o = 2\pi f = \frac{c\nu_{01}}{a}$$

$$f = \frac{2.405 c}{2\pi a}$$

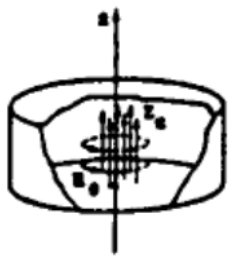


Example: radius of resonator for $f = 201.25$ MHz:

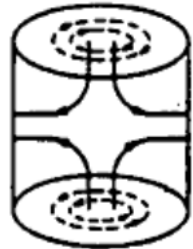
$$a = \frac{2.405 c}{2\pi f} = 0.57 m$$

TM_{010} mode in a pill-box cavity.

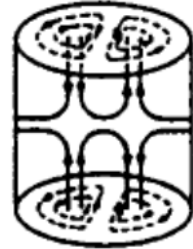
TM-Modes in Cylindrical Resonator



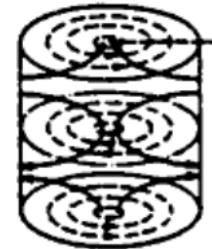
TM₀₁₀ mode



TM₀₁₁ mode

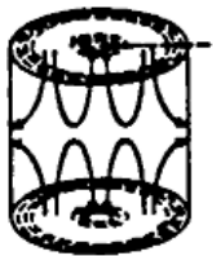


TM₁₁₁ mode

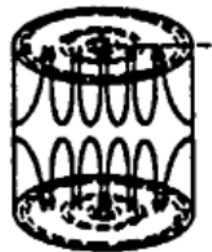


TM₀₁₂ mode

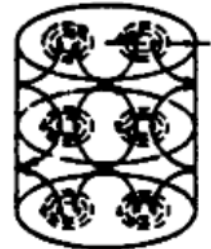
E ———
H - - - -



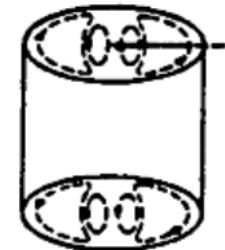
TM₀₂₁ mode



TM₀₃₁ mode



TM₁₁₂ mode



TM₁₂₁ mode

TM-mode field patterns in cylindrical resonator (T.Wangler, LA-UR-93-805).

TE_{nmp} Modes in Cylindrical Cavity

Field components of TE_{nmp} modes in cylindrical cavity

$$H_z = H_o J_n(\chi r) \cos n\theta \sin \chi_z z$$

$$H_r = H_o \frac{\chi_z}{\chi} J_n'(\chi r) \cos n\theta \cos \chi_z z$$

$$H_\theta = -H_o \frac{n\chi_z}{\chi^2 r} J_n(\chi r) \sin n\theta \cos \chi_z z$$

$$E_z = 0$$

$$E_r = iH_o \frac{n\omega_o \mu_o}{\chi^2 r} J_n(\chi r) \sin n\theta \sin \chi_z z$$

$$E_\theta = iH_o \frac{\omega_o \mu_o}{\chi} J_n'(\chi r) \cos n\theta \sin \chi_z z$$

$$\chi_z = \frac{\pi p}{L}$$

Boundary condition:

$$E_\theta(a) = 0$$

$$J_n'(\chi a) = 0 \quad \chi = \frac{v_{nm}'}{a}$$

v_{nm}' is the root of equation $J_n'(x) = 0$

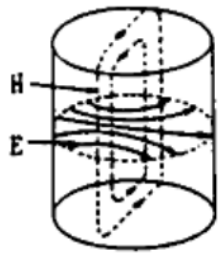
Frequency of TE_{nmp} oscillations

$$\omega_o = c \sqrt{\frac{v_{nm}'^2}{a^2} + \left(\frac{\pi p}{L}\right)^2}$$

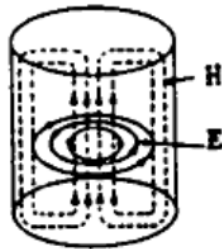
Zeros v_{nm}' of equation $J_n'(x) = 0$

	$m = 1$	$m = 2$	$m = 3$	$m = 4$
$n = 0$	3.832	7.016	10.173	13.324
$n = 1$	1.841	5.331	8.536	11.706
$n = 2$	3.054	6.706	9.969	13.170
$n = 3$	4.201	8.015	11.346	

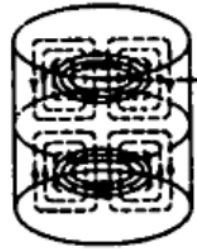
TE-Modes in Cylindrical Resonator



TE_{111} mode



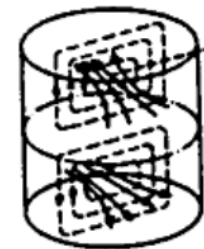
TE_{011} mode



TE_{012} mode



TE_{021} mode



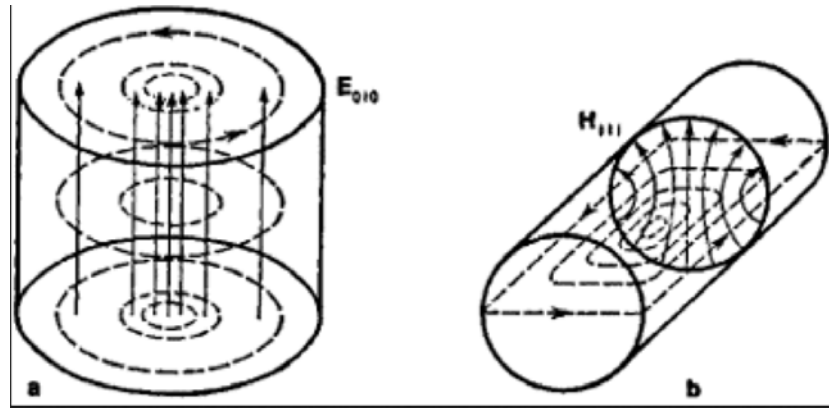
TE_{112} mode



TE_{121} mode

TE-mode field patterns in cylindrical resonator (T.Wangler, LA-UR-93-805).

Fundamental Modes of Cylindrical Resonator



Oscillations TE₁₁₁ and TM₀₁₀ are fundamental modes which frequencies coincide if

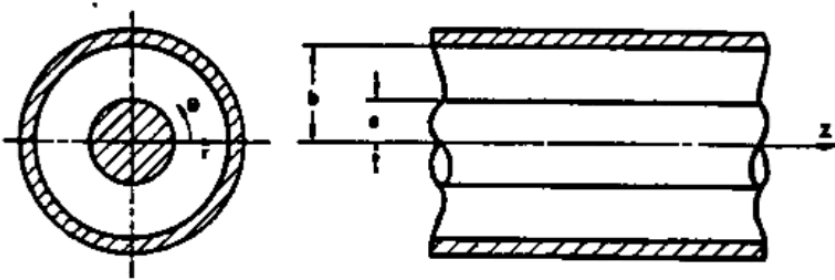
$$\frac{v_{01}^2}{a^2} = \frac{v_{11}^2}{a^2} + \left(\frac{\pi}{L}\right)^2$$

In this case of ratio of length of resonator to radius L/a is

$$\frac{L}{a} = \frac{\pi}{\sqrt{v_{01}^2 - v_{11}^2}} = 2.03$$

For long cylinder $L/a > 2.03$ the fundamental mode is TE₁₁₁ while for “flat” resonator $L/a < 2.03$ the fundamental mode is TM₀₁₀.

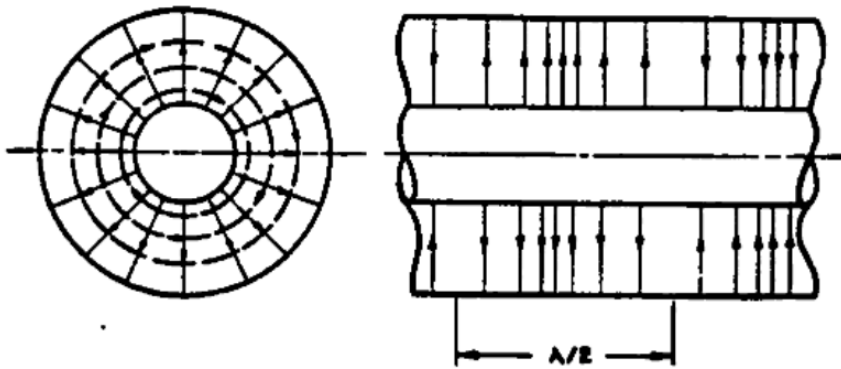
Coaxial Line



A section of coaxial transmission line

Field components of TEM wave propagating in coaxial transmission line

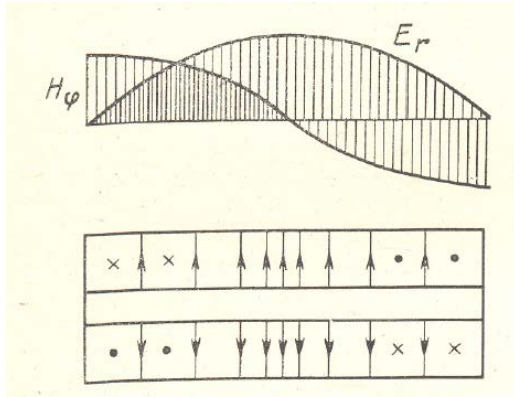
$$B_{\theta} = \frac{\mu_0 I}{2\pi r} \exp[i(\omega t - k_z z)]$$



Field distribution for the principal mode in coaxial line

$$E_r = \sqrt{\frac{\mu_0}{\epsilon_0}} \frac{I}{2\pi r} \exp[i(\omega t - k_z z)]$$

Half and Quarter Wave Resonators

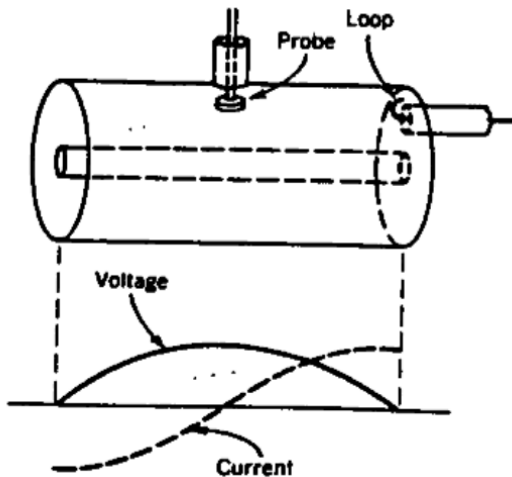


Resonance condition: $L = \frac{p\lambda}{2}$

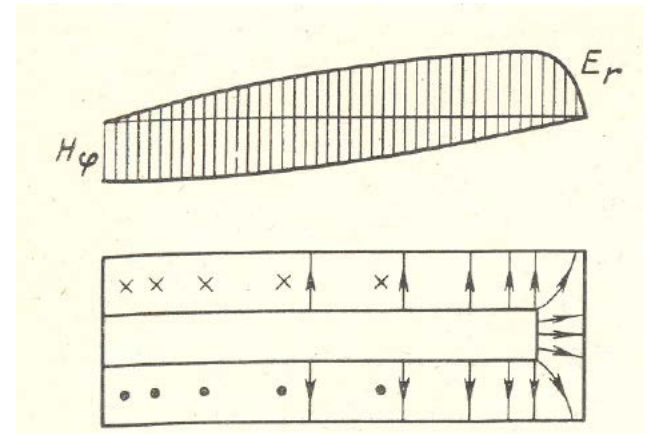
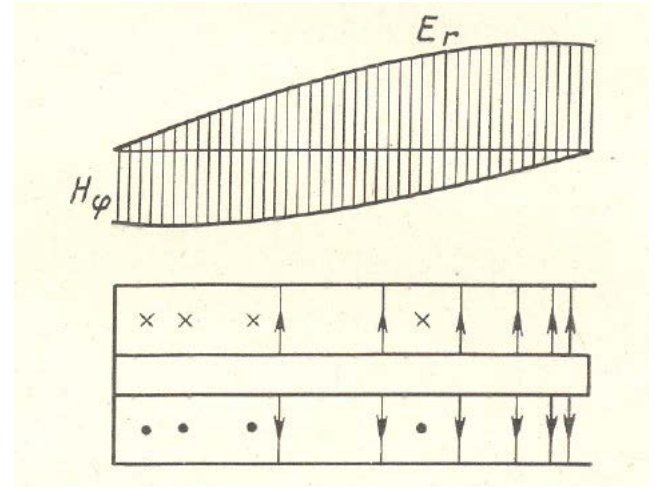
Component of RF field

$$B_{\theta} = \frac{\mu_0 I}{2\pi r} \cos\left(\frac{\pi p z}{L}\right) \cos \omega t$$

$$E_r = \sqrt{\frac{\mu_0}{\epsilon_0}} \frac{I}{2\pi r} \sin\left(\frac{\pi p z}{L}\right) \sin \omega t$$



Coaxial resonator with voltage and current standing waves.



Quarter wave resonator

Conservation of Energy of Electromagnetic Field (Poynting's Theorem)

From Maxwell's equations:

$$\vec{H} \operatorname{rot} \vec{E} = -\vec{H} \frac{\partial \vec{B}}{\partial t} \quad \vec{E} \operatorname{rot} \vec{H} = \vec{E} \frac{\partial \vec{D}}{\partial t} + \vec{j} \vec{E}$$

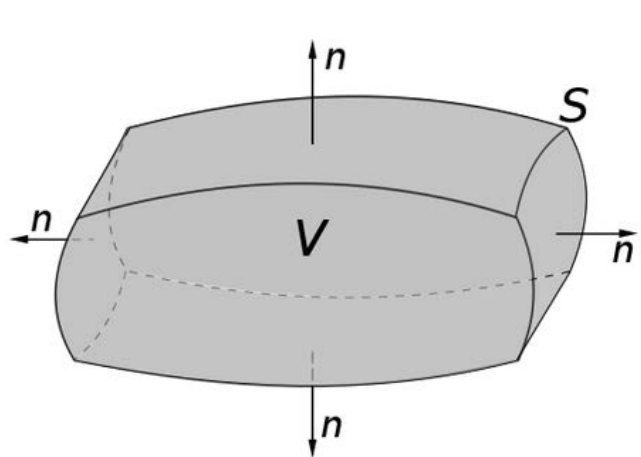
$$\vec{H} \operatorname{rot} \vec{E} - \vec{E} \operatorname{rot} \vec{H} = -\vec{H} \frac{\partial \vec{B}}{\partial t} - \vec{E} \frac{\partial \vec{D}}{\partial t} - \vec{j} \vec{E}$$

From vector analysis equity:

$$\vec{H} \operatorname{rot} \vec{E} - \vec{E} \operatorname{rot} \vec{H} = \operatorname{div}[\vec{E}, \vec{H}]$$

Therefore

$$\operatorname{div}[\vec{E}, \vec{H}] = -\vec{H} \frac{\partial \vec{B}}{\partial t} - \vec{E} \frac{\partial \vec{D}}{\partial t} - \vec{j} \vec{E}$$



A region V bounded by the surface $S = \partial V$ with the surface normal \mathbf{n}

Gauss Theorem:

$$\iiint_V (\nabla \cdot \mathbf{F}) dV = \iint_S (\mathbf{F} \cdot \mathbf{n}) dS.$$

Conservation of Energy of Electromagnetic Field (Poynting's Theorem) (cont.)

Application of Gauss Theorem gives:

$$\oint_S [\vec{E}, \vec{H}] d\vec{S} = - \int_V \left(\vec{H} \frac{\partial \vec{B}}{\partial t} + \vec{E} \frac{\partial \vec{D}}{\partial t} \right) dV - \int_V \vec{j} \vec{E} dV$$

Calculating terms

$$\vec{H} \frac{\partial \vec{B}}{\partial t} = \mu_o \vec{H} \frac{\partial \vec{H}}{\partial t} = \frac{\partial}{\partial t} \left(\frac{\mu_o H^2}{2} \right)$$

$$\vec{E} \frac{\partial \vec{D}}{\partial t} = \epsilon_o \vec{E} \frac{\partial \vec{E}}{\partial t} = \frac{\partial}{\partial t} \left(\frac{\epsilon_o E^2}{2} \right)$$

Change of energy of electromagnetic field in volume V:

$$\int_V \left(\vec{H} \frac{\partial \vec{B}}{\partial t} + \vec{E} \frac{\partial \vec{D}}{\partial t} \right) dV = \frac{1}{2} \frac{d}{dt} \left[\int_V (\mu_o H^2 + \epsilon_o E^2) \right]$$

Electromagnetic energy:

$$W = \frac{1}{2} \int_V (\mu_o H^2 + \epsilon_o E^2)$$

The rate of energy transfer from a region of space equals the rate of work done on a charge distribution plus the energy flux leaving that region.

$$\oint_S [\vec{E}, \vec{H}] d\vec{S} = - \frac{d}{dt} \int_V \left(\frac{\mu_o H^2}{2} + \frac{\epsilon_o E^2}{2} \right) dV - \int_V \vec{j} \vec{E} dV$$

Energy Dissipation in Resonator and Quality Factor

Dissipated power is a combination of power losses inside cavity and outside cavity

$$P = P_o + P_{ext}$$

Energy stored in cavity

$$W_o = \frac{1}{2} \int_{V_o} \mu H_m^2 dV = \frac{1}{2} \int_{V_o} \epsilon E_m^2 dV$$

Quality factor

$$Q = \frac{\omega_o W_o}{P}$$

Q-factor is a combination of unloaded quality factor of cavity and external quality (loaded Q factor)

$$\frac{1}{Q} = \frac{1}{Q_o} + \frac{1}{Q_{ext}}$$

External quality factor

$$Q_{ext} = \frac{\omega_o W_o}{P_{ext}}$$

Losses in metal with surface resistance R_s [Ohm]

$$P_o = \frac{R_s}{2} \int_S H_m^2 dS$$

Unloaded quality factor

$$Q_o = \frac{\omega_o W_o}{P_o}$$

$$Q_o = \frac{\omega_o \mu_o \int_V H_m^2 dV}{R_s \int_S H_m^2 dS}$$

Unloaded Quality Factor of TM_{010} Cavity

Magnetic field

$$H_{m\theta} = -E_o \sqrt{\frac{\epsilon_o}{\mu_o}} J_1(v_{01} \frac{r}{a})$$

Energy stored in cavity

$$W_o = \frac{1}{2} \int_{V_o} \mu_o H_{m\theta}^2 dV = \frac{\pi \epsilon_o E_o^2 L a^2 J_1^2(v_{01})}{2} = 0.135 \pi \epsilon_o L a^2 E_o^2$$

Loss power in cavity

$$P_o = \frac{R_s}{2} \int_S H_{m\theta}^2 dS = \pi a R_s E_o^2 \frac{\epsilon_o}{\mu_o} J_1^2(v_{01})(L + a)$$

Unloaded quality factor

$$Q_o = \frac{\omega_o W_o}{P} = \frac{v_{01}}{2R_s} \sqrt{\frac{\mu_o}{\epsilon_o}} \frac{1}{(1 + \frac{a}{L})} = 1.2025 \frac{376.7 [Ohm]}{R_s} \frac{1}{(1 + \frac{a}{L})}$$

Unloaded Quality Factor of Coaxial Resonator

Azimuthal magnetic field

$$H_{m\theta} = \frac{I_m}{2\pi r} \cos \frac{p\pi z}{L}$$

Integral over volume

$$\int_{V_o} H_m^2 dV = \pi L \left(\frac{I}{2\pi}\right)^2 \ln \frac{R_2}{R_1}$$

Integral over surface

$$\int_{V_o} H_m^2 dS = \pi \left(\frac{I}{2\pi}\right)^2 \left[4 \ln \frac{R_2}{R_1} + L \left(\frac{1}{R_1} + \frac{1}{R_2}\right)\right]$$

Quality factor

$$Q_o = \frac{p\pi}{R_s} \sqrt{\frac{\mu_o}{\epsilon_o}} \frac{\ln \frac{R_2}{R_1}}{4 \ln \frac{R_2}{R_1} + L \left(\frac{1}{R_1} + \frac{1}{R_2}\right)}$$

Filing Time of Resonator

Power losses is a rate of decrease of stored energy

$$P = -\frac{dW_o}{dt}$$

Substitution into equation $Q = \frac{\omega_o W_o}{P}$ gives equation for decrease of stored energy

$$\frac{dW_o}{dt} = -\frac{\omega_o W_o}{Q}$$

Solution

$$W_o = W_o(0)e^{-\frac{\omega_o t}{Q}}$$

Electrical field changes with two times smaller rate:

$$\alpha = \frac{\omega_o}{2Q}$$

Electric field

$$E = E_m e^{i\omega_o t} e^{-\frac{\omega_o t}{2Q}}$$

Filing time of the cavity

$$t_f = \frac{2Q}{\omega_o}$$

Complex frequency of cavity

$$\dot{\omega}_o = \omega_o \left(1 + i \frac{1}{2Q}\right)$$

Filing Time of Resonator (cont.)

When the power source is matched to the resonant structure through a coupling loop, such that no power is reflected toward the source, then the loaded Q

$$Q = \frac{Q_o}{1 + \beta}$$

where β is the coupling coefficient. For negligible beam current $\beta = 1$.

The filling time becomes

$$t_f = \frac{2Q}{\omega_o} = \frac{2Q_o}{\omega_o(1 + \beta)}$$

During the filling time, the transient effect exists when reflected power cannot be avoided.

Shunt Impedance

Shunt impedance is a ratio of effective voltage in resonator to dissipated power. The higher shunt impedance, the larger accelerating field is generated per same power

$$R_{sh} = \frac{U^2}{P} [\Omega]$$

Effective shunt impedance

$$R = \frac{(UT)^2}{P} = R_{sh} T^2 [\Omega]$$

Often shunt impedance per unit length is used:

$$Z = \frac{U^2}{PL} = \frac{E_o^2}{(P/L)} [\Omega / m]$$

Effective shunt impedance per unit length

$$ZT^2 = \frac{R}{L} = \frac{(E_o T)^2}{(P/L)} [\Omega / m]$$

Ratio R over Q (depends on geometry only)

$$\frac{R}{Q} = \frac{(UT)^2}{\omega_o W_o}$$

Shunt Impedance Versus Frequency

RF power loss per unit length is proportional to the product of the square of the wall current and the wall resistance per unit length

$$\frac{dP}{dz} \sim I_w^2 R_w$$

Electric field is proportional to wall current divided by cavity radius

$$E_z \sim I_w / a$$

The wall resistance per unit length is equal to the resistivity of the wall material divided by the area of the surface through which the current is flowing

$$R_w = \frac{\rho_w}{2\pi a \delta}$$

Skin depth (μ is the permeability of the walls)

$$\delta = \sqrt{\frac{2\rho_w}{\omega_o \mu}}$$

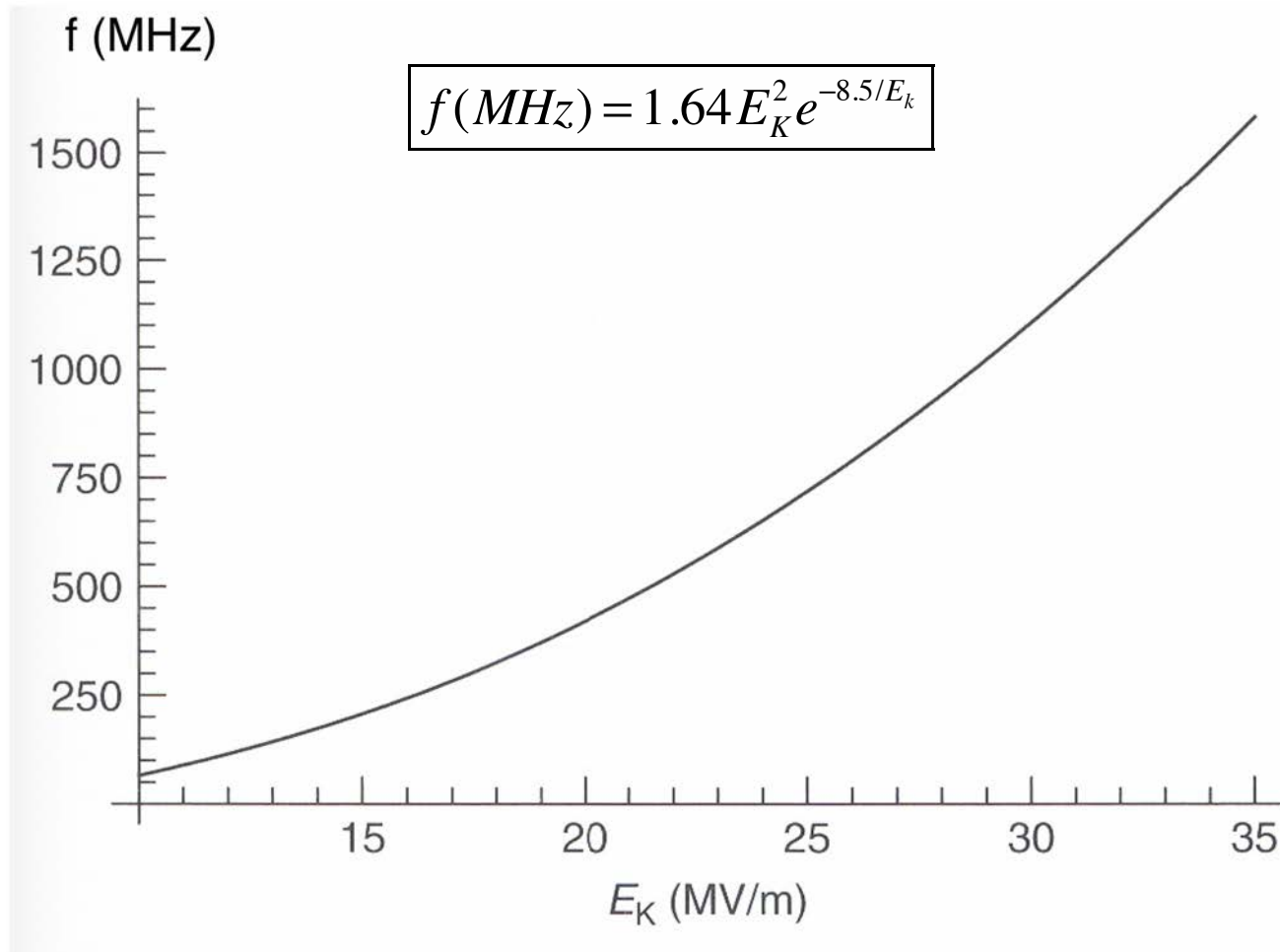
Taking into account that frequency is inversely proportional to frequency cavity radius,

$$\omega_o \sim \frac{1}{a}$$

the shunt impedance is proportional to square root of frequency. From viewpoint of RF power economy, it is better to operate at higher frequencies. However, aperture for the beam must be kept large enough.

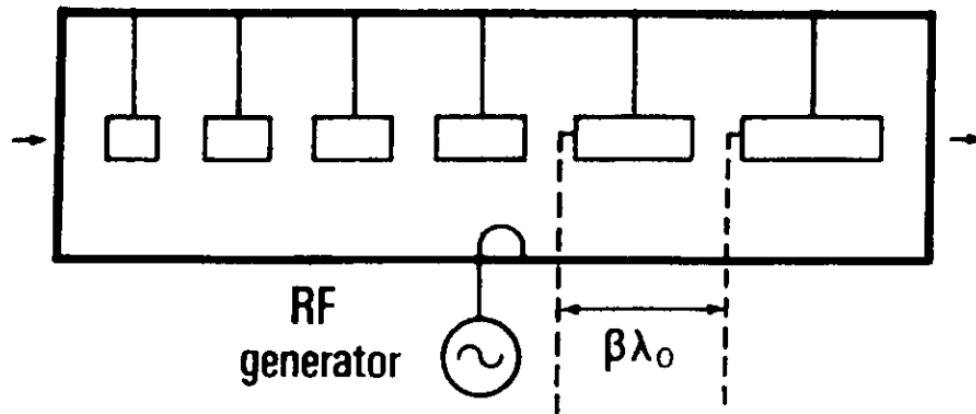
$$\frac{E_z^2}{\left(\frac{dP}{dz}\right)} \sim \frac{1}{a^2 R_w} \sim \frac{\delta}{a} \sim \sqrt{\omega_o}$$

Kilpatrick Limited RF Field

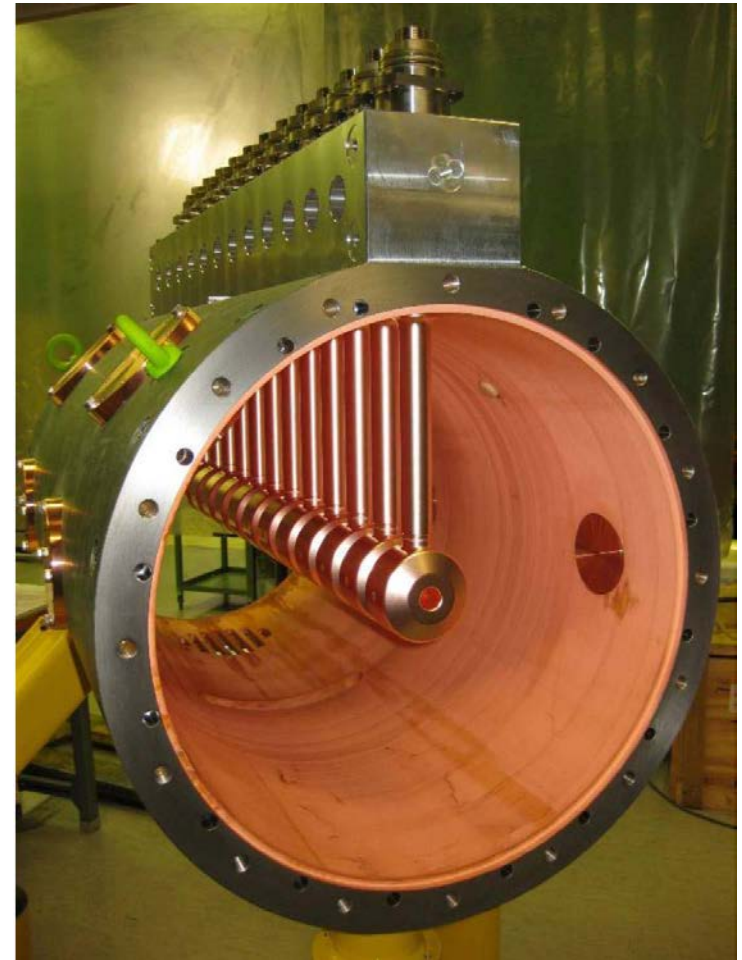


Kilpatrick limited RF field E_k [MV/m]

Alvarez Structure

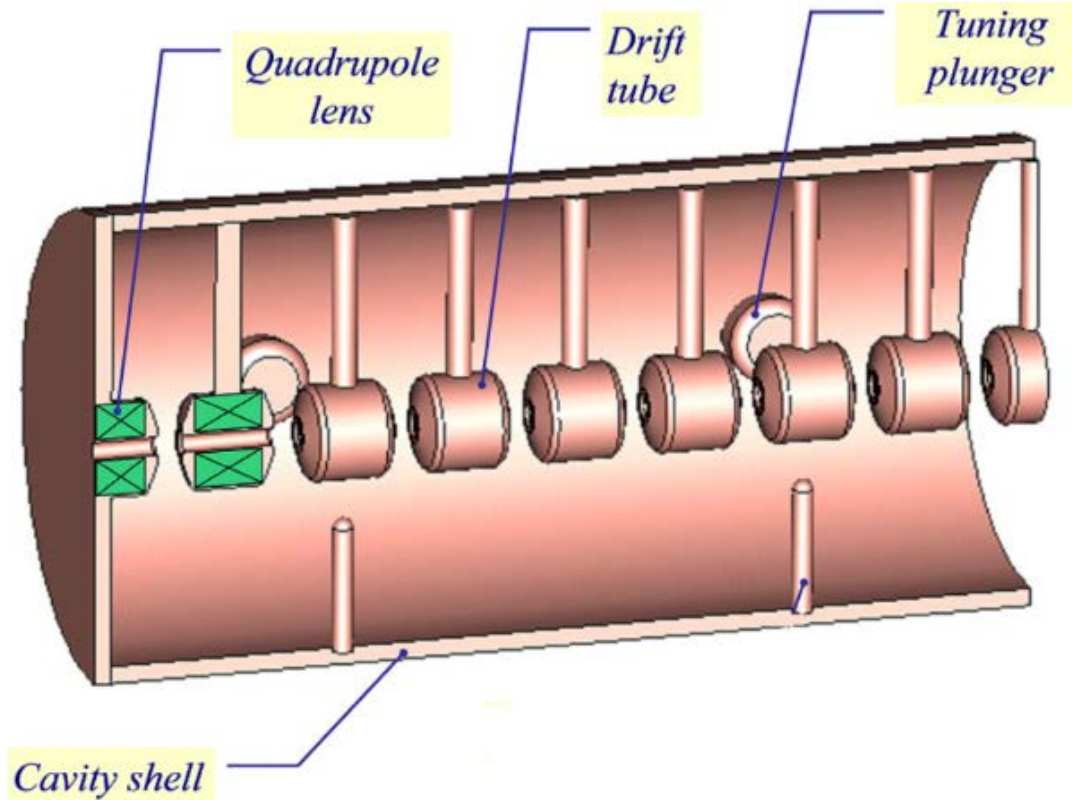


Alvarez structure is a cavity excited with TM₀₁₀ mode, loaded with drift tubes. Efficient for $0.04 < \beta < 0.5$. Field Distribution is sensitive to all deformations



Drift Tube Linac Prototype for CERN Linac4 (325 MHz). Quadrupoles are located inside drift tubes.

Alvarez Structure (cont.)



Tuning plungers are inserted for correct frequency under temperature variation. Post couplers are inserted to suppress unwanted modes.

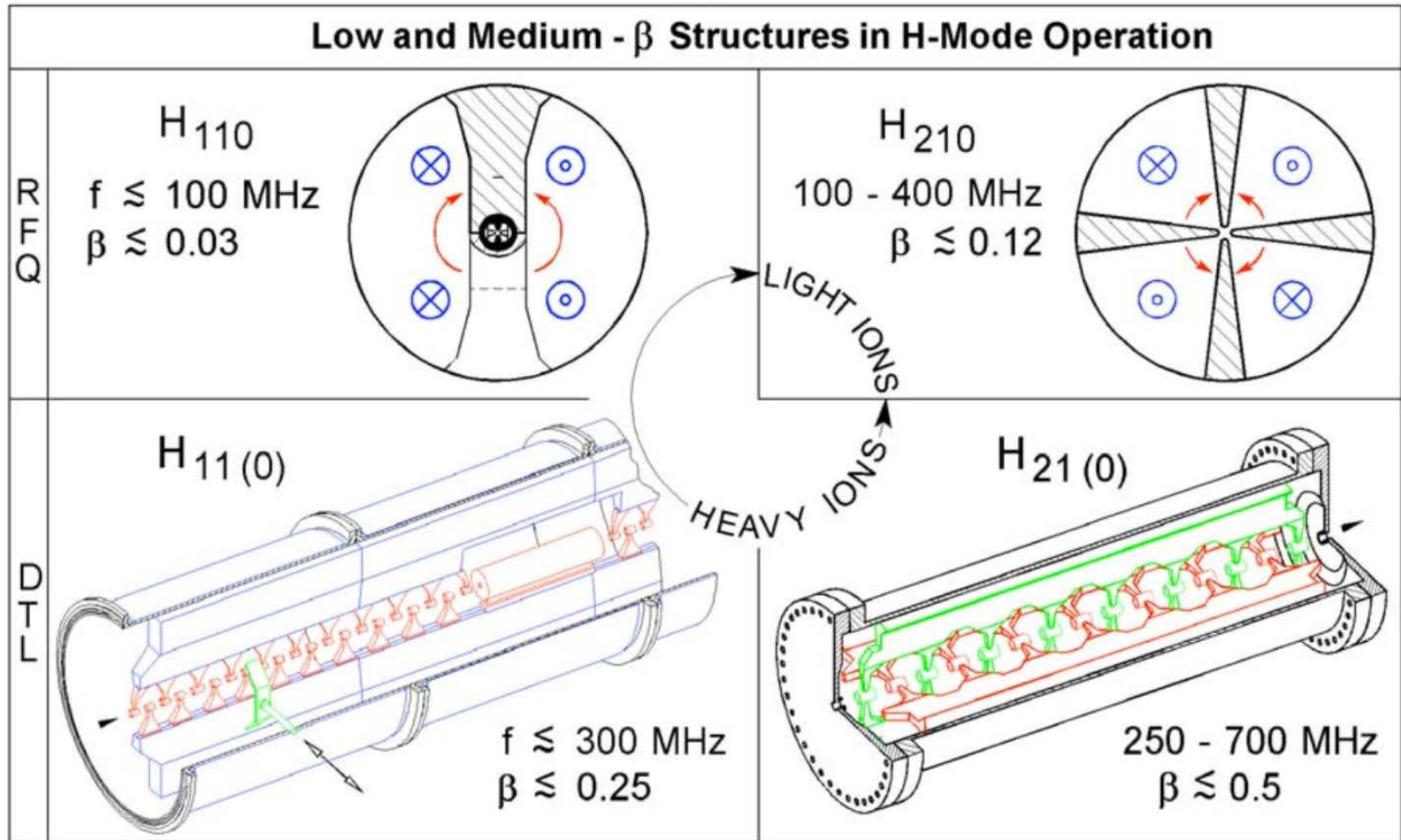
Parameters of LANL Alvarez Structures

Table 4.1 Drift-Tube Linac Parameters for the LAMPF Proton Accelerator

	Tank 1	Tank 2	Tank 3	Tank 4	
Cell No.	1 to 31	32 to 59	60 to 97	98 to 135	136 to 165
Energy in (MeV)	0.75	5.39		41.33	72.72
Energy out (MeV)	5.39	41.33		72.72	100.00
Δ energy (MeV)	4.64	35.94		31.39	27.28
Tank length (cm)	326.0	1968.8		1875.0	1792.0
Tank diameter (cm)	94.0	90.0		88.0	88.0
D. T. diameter (cm)	18.0	16.0		16.0	16.0
D. T. corner radius (cm)	2.0	4.0		4.0	4.0
Bore radius (cm)	0.75	1.0	1.5	1.5	1.5
Bore corner radius (cm)	0.5	1.0		1.0	1.0
G/L	0.21-0.27	0.16-0.32		0.30-0.37	0.37-0.41
Number of cells	31	66		38	30
Number of quads	32	29	38	20	16
Quad gradient (KG/cm)	8.34-2.46	2.44-1.89	1.01-0.87	0.90-0.84	0.84-0.83
Quad length (cm)	2.62-7.88	7.88	16.29	16.29	16.29
E_0 (MV/m)	1.60-2.30	2.40		2.40	2.50
φ_s (deg)	-26°	-26°		-26°	-26°
Power (MW)	0.305	2.697		2.745	2.674
Intertank space (cm)	15.90	85.62		110.95	--

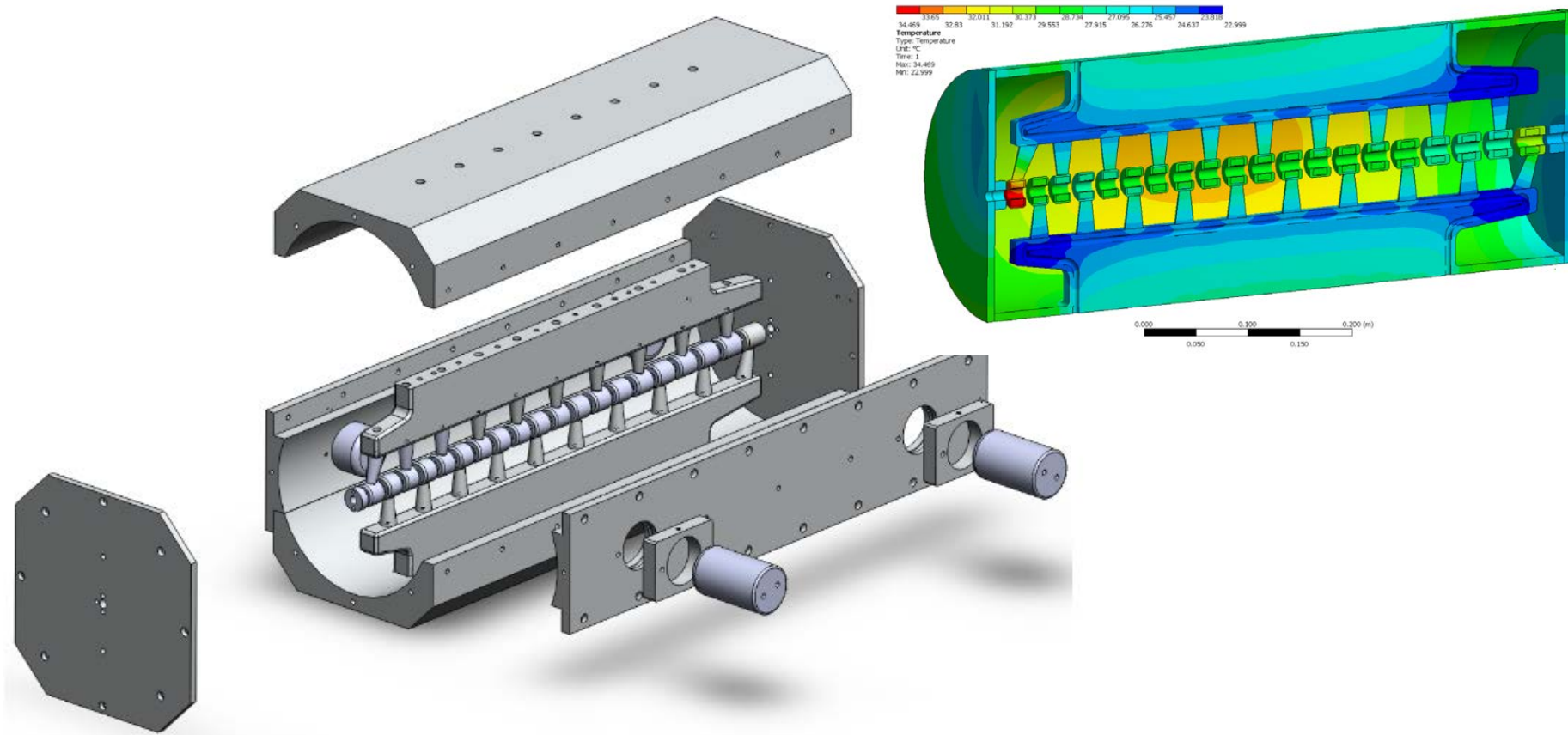
Total length including intertank spaces = 6174.281 cm. (202 ft. 6.819 in.)

H - Resonators



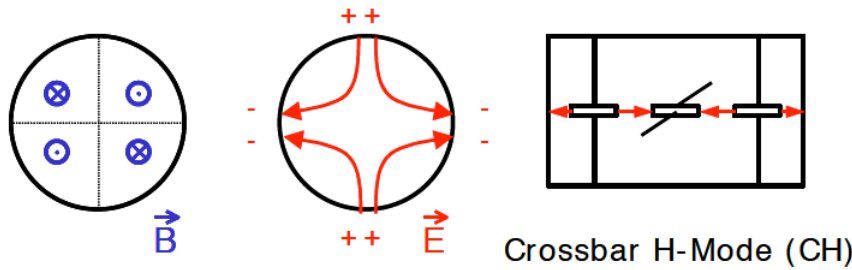
H-type accelerating structures (U.Ratzinger, 2005).

Interdigital H-Mode Structure

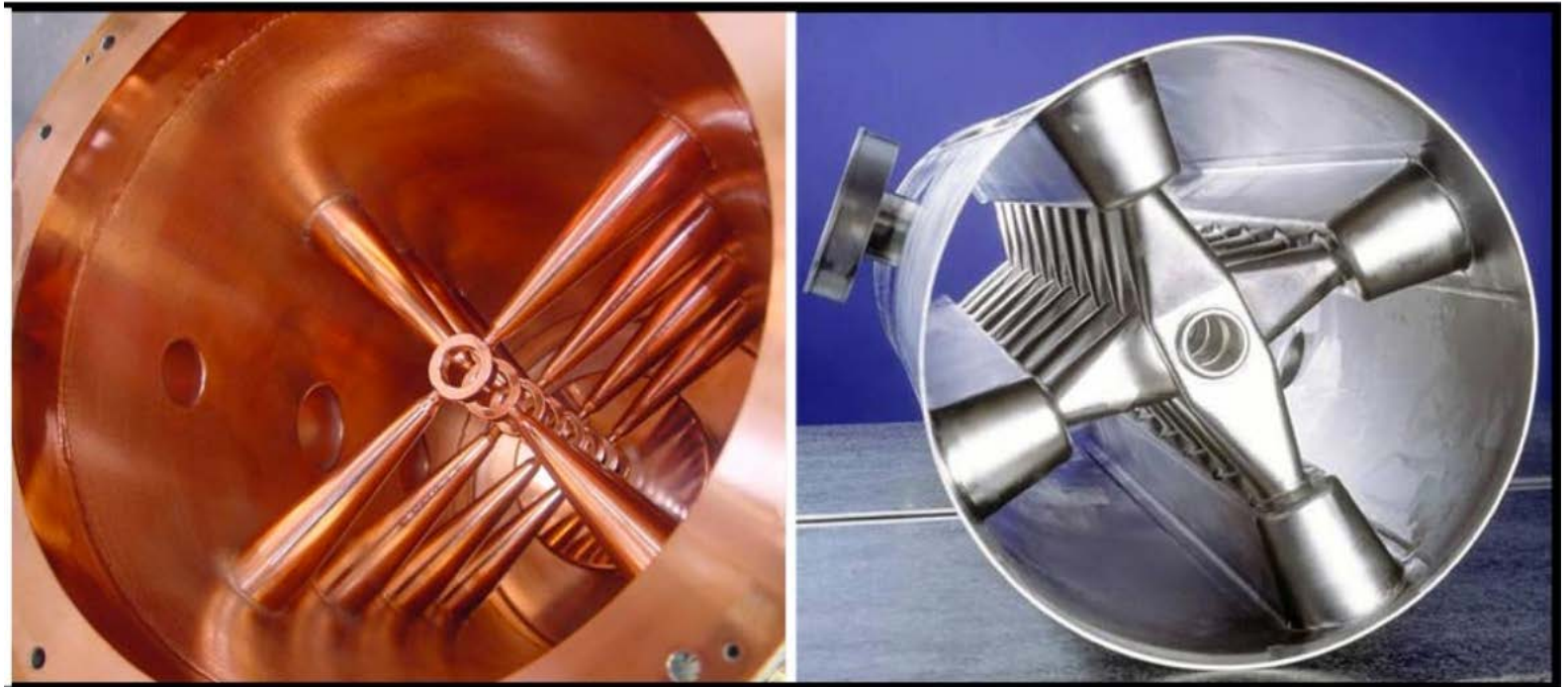


H-Mode Accelerating Structure with Permanent Magnet Quadrupole Beam Focusing (S.Kurennoy et al, 2011).

Cross-Bar (CH) Structures

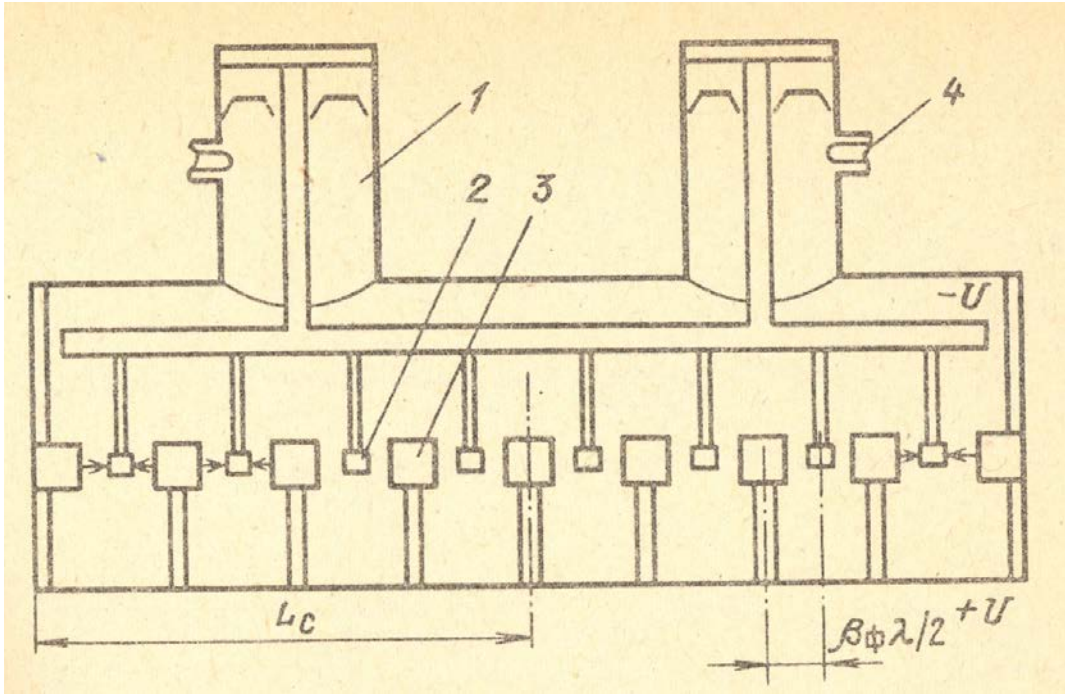
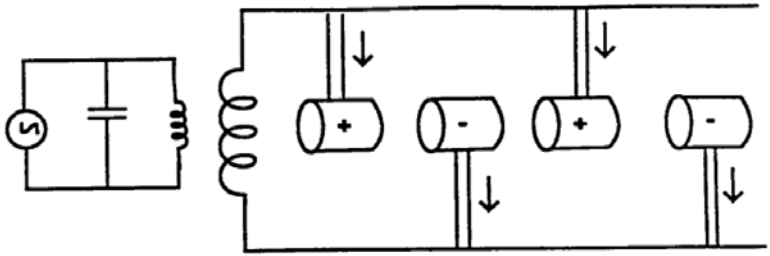


Field pattern in H_{211} cavity
(M. Vretenar, 2012)



350 MHz room temperature CH-DTL and 350 MHz superconducting CH-DTL structure (H.Podlech et al, 2007).

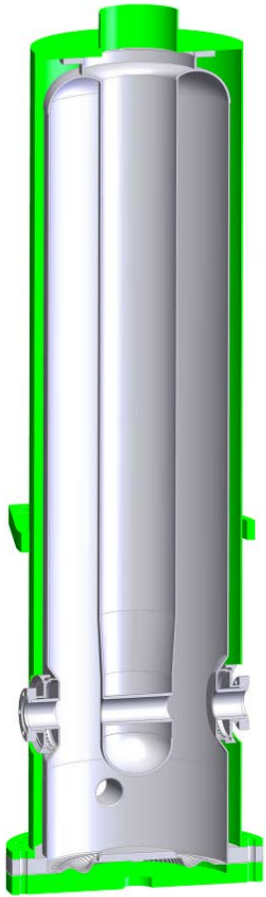
Wideroe Structure



Original idea: the voltages are supplied to the electrodes by alternately connecting them to two conductors parallel to the beamline and driven by a high-frequency oscillator.

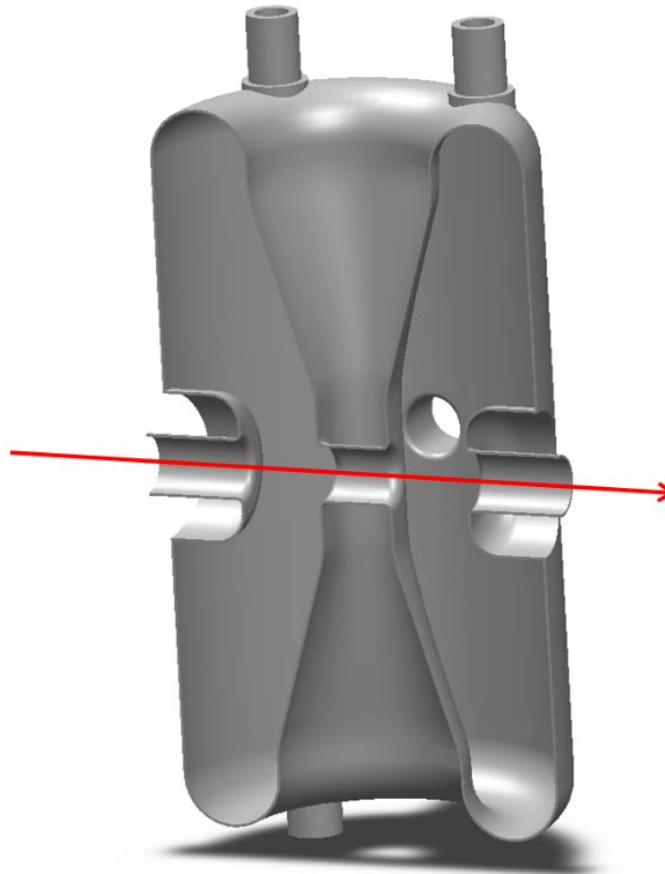
Wideroe structure made of coaxial line: external cylinder is used as one of the line, while internal conductor is used as a second line.

Independently Phased Cavities

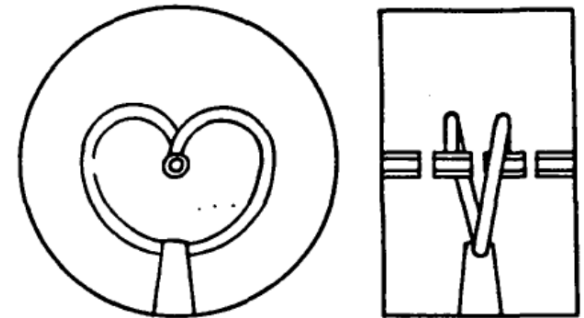


10 cm
└───┘

Quarter-wave resonator.

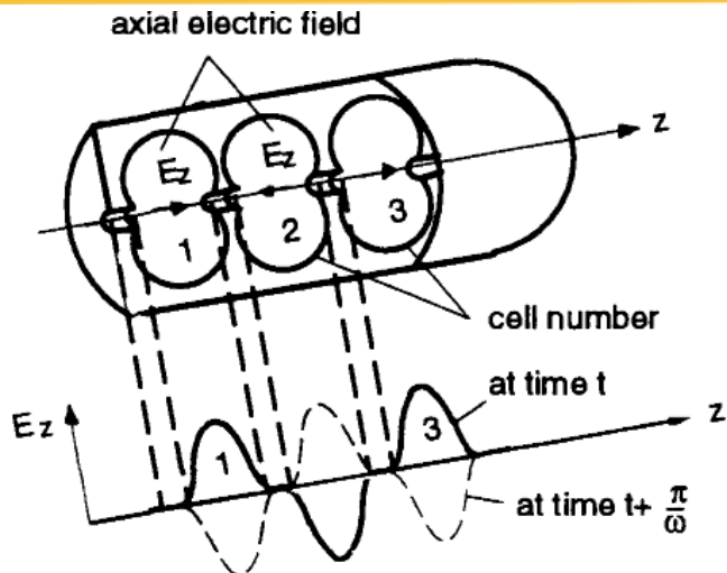


Half-wave resonator.



Superconducting splitting niobium resonator (ANL).

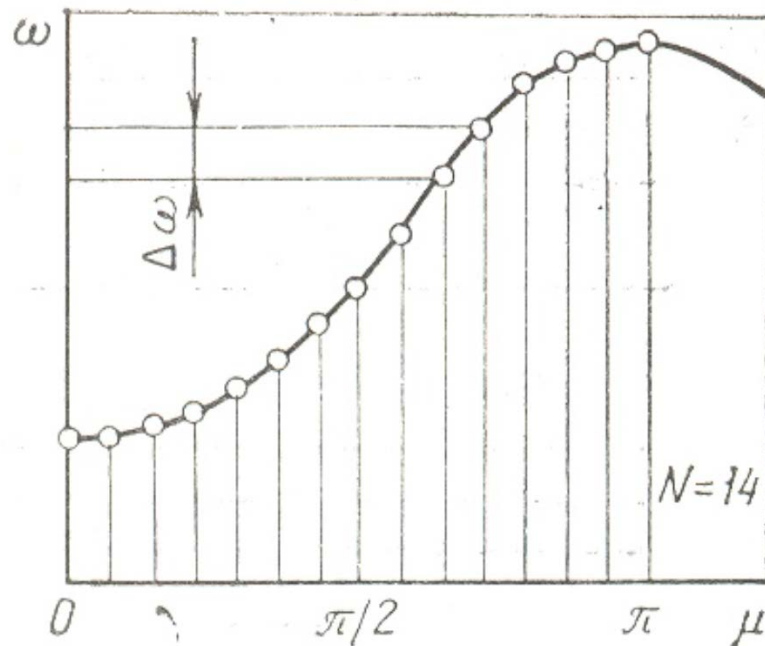
Coupled Cells



Standing wave accelerator operating in the π - mode.

The whole structure can be considered as a one resonator working on $\mu' = \pi p$ ($p = 0, 1, 2, \dots$) mode. On the other hand, in a resonator with N cells $\mu' = \mu N$ where μ is the phase shift between cells. Therefore, phase shift between cells:

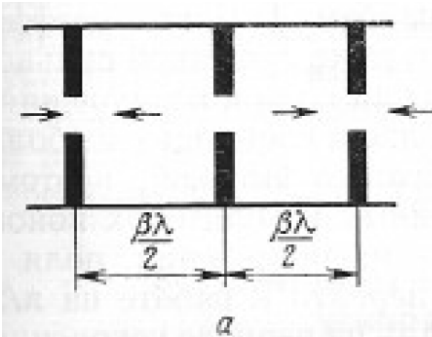
$$\mu = p \frac{\pi}{N} \quad p = 0, 1, 2, \dots$$



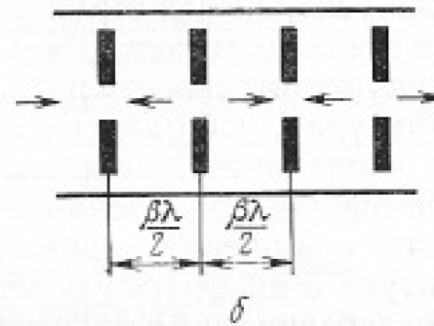
Dispersion curve of coupled cell structure: in a structure containing N elements there are $N+1$ modes of oscillations.

Coupled Cells (cont.)

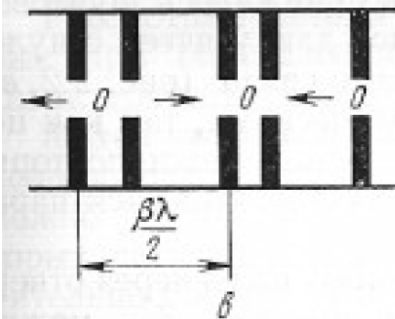
Disk-loaded waveguide working on π -mode: weak coupling, sensitive to instability



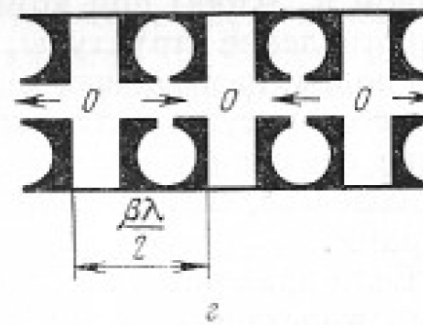
Disk-loaded π -mode waveguide with additional magnetic coupling



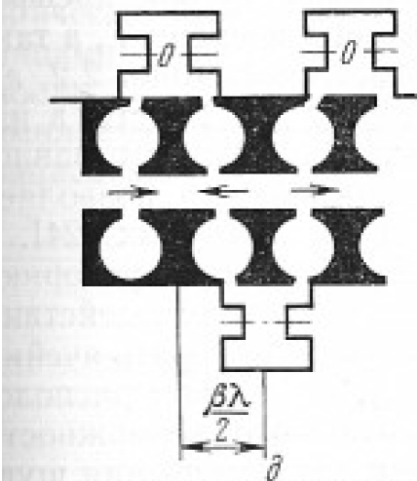
Better coupling



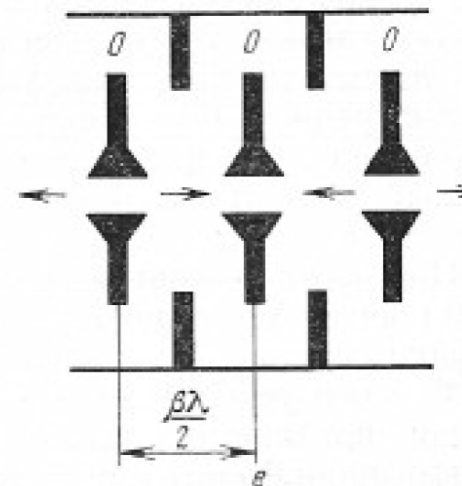
Bi-periodic structures



Side-coupled structure



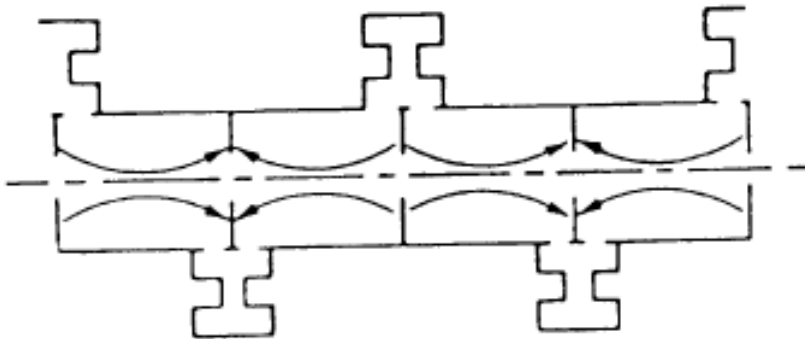
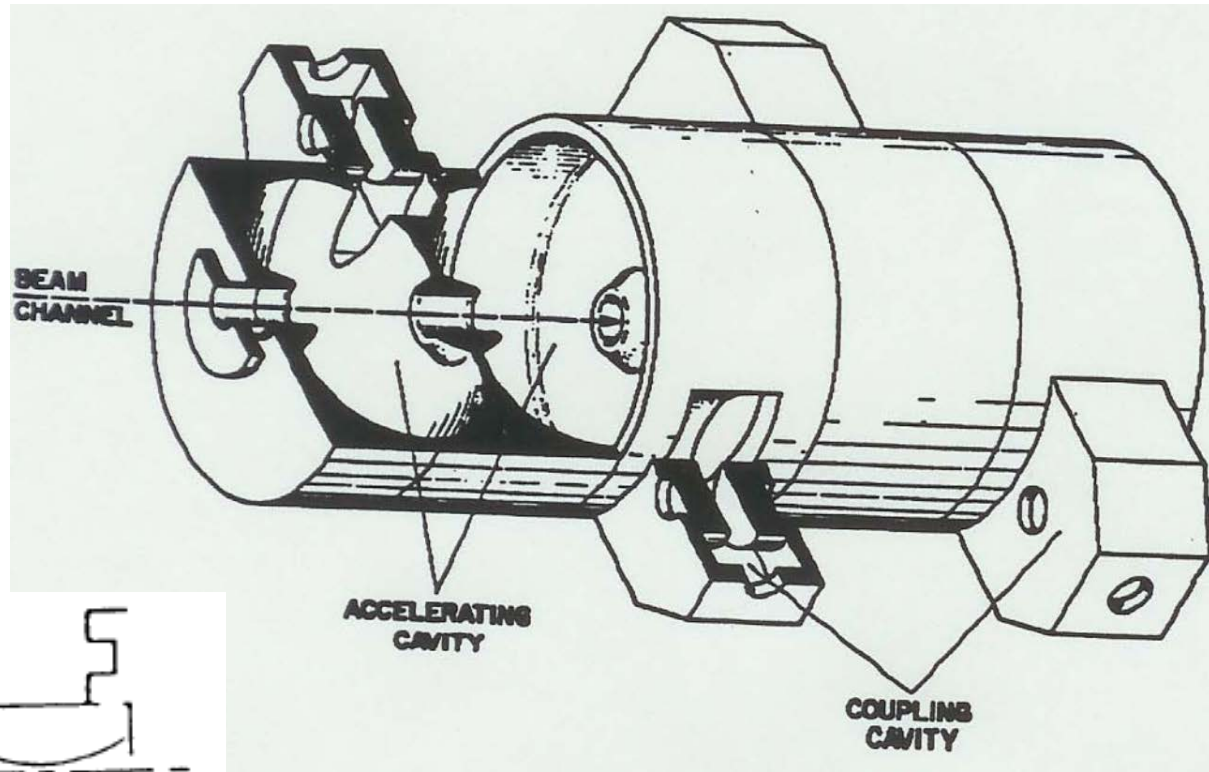
Disk and washer structure



Side-Coupled Cavities

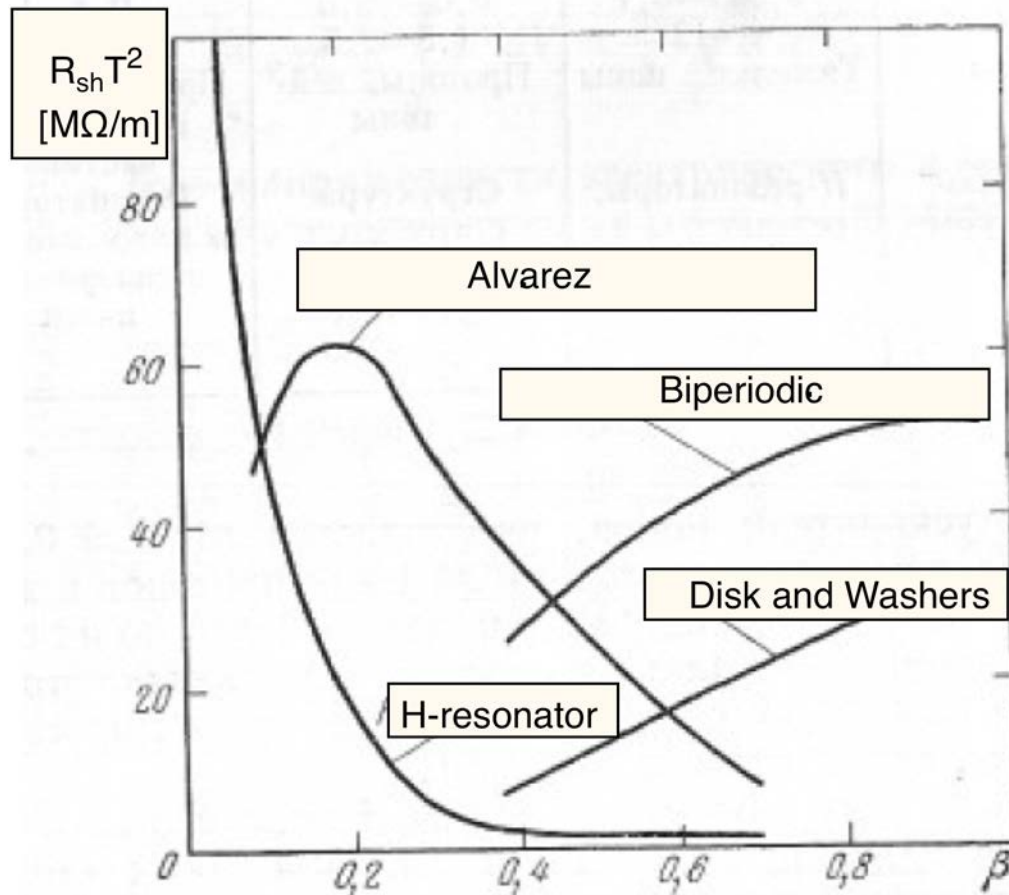
Energy range: 100-
800 MeV

High shunt
Impedance: 50 M Ω /m



Los Alamos Side Coupled Structure.

Shunt Impedance of Accelerating Structures



Shunt impedance of accelerating structure versus velocity β .

Elliptical Superconducting Multi-Cell Cavities

High gradient:
10-20 MV/m
Compact design
Large aperture

Chain of cells
electrically
coupled (ZT^2 is
not a concern)

Lower RF power
requirement



Six-cell 805-MHz medium-beta ($\beta=0.61$) and high-beta ($\beta=0.81$) superconducting niobium elliptical cavities. The SNS linac contains about 80 niobium cavities.